

# The electrical conductivity of upper-mantle rocks: water content in the upper mantle

Duojun Wang · Heping Li · Li Yi · Baoping Shi

Received: 27 February 2007 / Accepted: 21 November 2007 / Published online: 7 December 2007  
© Springer-Verlag 2007

**Abstract** The electrical conductivity of upper-mantle rocks—dunite, pyroxenite, and lherzolite—was measured at  $\sim 2\text{--}3$  GPa and  $\sim 1,273\text{--}1,573$  K using impedance spectra within a frequency range of  $0.1\text{--}10^6$  Hz. The oxygen fugacity was controlled by a Mo–MoO<sub>2</sub> solid buffer. The results indicate that the electrical conductivity of lherzolite and pyroxenite are approximately half and one order of magnitude higher than that of dunite, respectively. A preliminary model involving water and iron content effects on the electrical conductivity was derived and is summarized by the relation:

$$\sigma = 10^{5.2 \pm 0.4} C_w^{0.67 \pm 0.07} \exp\left(-\frac{(183 \pm 9)\text{kJ/mol}}{RT}\right) \times \exp\left(X \frac{(79 \pm 3)\text{kJ/mol}}{RT}\right).$$

The results also indicate that pyroxenes dominate the bulk conductivity of upper mantle in hydrous conditions and suggest the maximum water content in oceanic upper mantle is as high as  $\sim 0.09$  wt%.

**Keywords** Electrical conductivity · Upper mantle · Water content

## Introduction

Substantial amounts of water can be dissolved into the nominally anhydrous minerals (NAMS), such as the olivine and pyroxenes as hydrogen defects (Bell and Rossman 1992; Bai and Kohlstedt 1992; Kohlstedt et al. 1996); therefore, the upper mantle may contain large amounts of water. Water dramatically affects both the physical and chemical properties of minerals and rocks, and plays an important role in the dynamics and evolution of earth's mantle. Consequently, estimating the distribution of water in the mantle has been an important issue in geophysics and geochemistry (Williams and Hemley 2001; Karato 2003; Huang et al. 2005; Wang et al. 2006).

Electrical conductivity is sensitive to water, and therefore it can be used as a sensor for water content with high confidence (Karato 2006). Recently, several researchers have estimated the water content in the transition zone (Huang et al. 2005) and the upper mantle (Wang et al. 2006; Yoshino et al. 2006) by electrical conductivity methods. However, they may underestimate the water content in the transition zone and upper mantle because they simply assume that the electrical conductivity is dominated by olivine (in the upper mantle) and wadsleyite or ringwoodite (in the transition zone). However, other coexisting phases such as pyroxene and its high-pressure polymorphs may also contribute to the bulk conductivity of the mantle. Olivine is the volumetrically dominant mineral in the upper mantle (Ringwood 1975; Irifune and Ringwood 1987), but pyroxene stores considerably more H<sub>2</sub>O than olivine (for a review see Hirschmann et al. 2005).

---

D. Wang · H. Li (✉)  
Institute of Geochemistry,  
Chinese Academy of Sciences,  
Guiyang 550002, China  
e-mail: li-heping@hotmail.com

D. Wang · B. Shi  
Lab of Computational Geodynamics,  
Graduate University of Chinese Academy of Sciences,  
Beijing 100049, China

L. Yi  
Institute of Earthquake Science,  
China Earthquake Administration,  
Beijing 100036, China

Therefore, pyroxenes should markedly affect bulk conductivity whose electrical conductivity is dominated by water-related defects.

Dunite, lherzolite, and pyroxenite are thought to be the primary rock types in the upper mantle, therefore, knowledge of the electrical properties of hydrous rocks at high pressures and temperatures may provide us with a clue to the water content in the upper mantle.

In this article, we report the electrical conductivity results of dunite, pyroxenite, and lherzolite under controlled thermodynamic conditions, and determine the iron and water effects on the electrical conductivity of these rocks. The water content in the upper mantle was inferred by comparison between the experimental data and geophysical observations.

## Experiments

### Sample preparation

The starting materials are natural dunite, pyroxenite, and lherzolite. The dunite was collected from Dengpa county (latitude between 82°00' E and 92°20' E and longitude between 27°23' N and 31°49' N), Tibet, China; with a grain size varies between 0.5 mm and 1.5 mm. Small amounts of serpentine were present at the edge of the sample. The pyroxenite and lherzolite xenoliths from Hannuoba basalt were collected from Wanquan county (latitude between 114°30' E and 115°00' E and longitude between 41°00' N and 31°50' N), HeBei province, China; their grain sizes are 0.5–1.5 mm and 0.5–1.0 mm, respectively. The lherzolite has an approximate modal composition of 25% orthopyroxene, 15% clinopyroxene, 58% olivine, and 2% spinel. The pyroxenite has an approximate modal composition of 50% orthopyroxene, 45% clinopyroxene, and 5% metal oxide. The location of xenoliths and the mineralogical chemical analyses are also shown by Xu et al. (2002) and Rudnick et al. (2004). We selected fresh rocks that we cored and polished into cylinders (the diameter ~6.0 mm, thickness ~5.0 mm) for electrical conductivity measurements. The major elements among these three rocks were determined by X-ray fluorescence spectroscopy. The results are shown in Table 1.

### Experimental methods

High-pressure experiments were conducted in the YJ-3000T press fitted with a wedge-type cubic anvil located at Institute of geochemistry, Chinese Academy of sciences. The detail of this apparatus has been described by Xu et al. (1994). The pressure is generated in a pyrophyllite cube

**Table 1** The chemical compositions of dunite, lherzolite, and pyroxenite

	Dunite	Lherzolite	Pyroxenite
Na <sub>2</sub> O	0.01	0.07	0.56
MgO	52.34	40.72	17.27
Al <sub>2</sub> O <sub>3</sub>	0.12	2.31	6.25
SiO <sub>2</sub>	41.36	44.79	48.08
P <sub>2</sub> O <sub>5</sub>	0.01	0.01	0.02
K <sub>2</sub> O	0.02	0.02	0.02
CaO	0.95	2.26	15.43
TiO <sub>2</sub>	0.01	0.08	0.62
MnO	0.04	0.13	0.15
Fe <sub>2</sub> O <sub>3</sub>	0.34	1.89	3.04
FeO	3.52	6.25	6.20
H <sub>2</sub> O <sup>+</sup>	0.46	1.28	1.58
CO <sub>2</sub>	0.08	0.13	0.21
X	0.039	0.101	0.545

*Note:* The major elements (in wt%) are determined by X-ray fluorescence spectrum; X is the molar ratio Fe/(Fe + Mg) of the three types of rocks

(original size is 32 mm) located at the center of the pressure cell and confined within six carbide square-surface anvils. The pressure generated in the cube was calibrated with melting curve of copper determined by the differential thermal analysis method (e.g., Akella and Kennedy 1971) and from the quartz–coesite transition series (e.g., Akimoto et al. 1977).

Figure 1 shows the sample assembly used for the electrical conductivity measurement. The pressure-transmitting pyrophyllite cube was formed from pyrophyllite powder, and the absorbed water in the pyrophyllite cubes was removed by heating the cube up to 800°C before the experiments. The furnace was made of stainless-steel foil. The sample (diameter ~6.0 mm, thickness ~5.0 mm), surrounded by alumina rings, was placed in the center of the furnace to minimize the temperature gradients. The

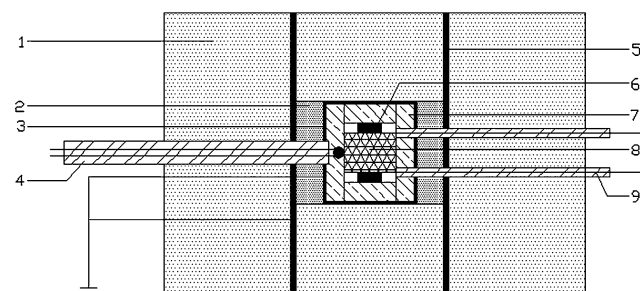


**Fig. 1** The sample assembly for electrical conductivity measurements at high pressure. (1) Pyrophyllite (baked to 1,073 K); (2) Pyrophyllite (baked to 1,273 K); (3) Mo shield; (4) Thermocouple; (5) Furnace; (6) Mo electrode; (7) Al<sub>2</sub>O<sub>3</sub> sleeve; (8) Sample; (9) Electric wire

temperature was measured by a NiCr–NiAl thermocouple that was placed next to the sample. Mo electrodes and Mo capsules in the sample assembly were used to keep the oxygen fugacity close to the Mo–MoO<sub>2</sub> buffer. The Mo capsule also used to minimize the noise and the leak current (for details see Xu et al. 1998).

The impedance spectroscopy technique has been used to study the electrical properties of minerals (e.g., Tyburczy and Roberts 1990; Roberts and Tyburczy 1991). The complex impedance  $Z^*$  of samples was determined with a Solartron 1260 Impedance/Gain phase Analyzer with 1 V applied voltage. Most experimental data was obtained within a frequency range between 0.1 and 1 MHz.

The real  $Z'$  and imaginary  $Z''$  parts of the complex impedance were obtained from the measurement of the magnitude,  $|Z|$ , and the phase angle,  $\theta$ , determined at a given frequency by the following two equations:

$$Z' = |Z| \cos \theta \tag{1}$$

$$Z'' = |Z| \sin \theta \tag{2}$$

Water contents of samples were measured after the electrical conductivity experiments. The concentration characteristics of the dissolved water (hydrogen) in the minerals within our specimens were determined using Fourier Transform Infrared (FTIR) spectroscopy (for methods see Bai and Kohlstedt 1992; Kohlstedt et al. 1996; Wang et al. 2006) at Yale University. The Paterson calibration (Paterson 1982) was used to calculate hydrogen content from infrared absorption. The bulk rock water contents were calculated from the water content of individual minerals within the rocks according to mineral assemblage. Water contents of the minerals within our specimens and bulk rock water contents are shown in Table 2.

### Results and discussion

Figure 2 shows the typical complex impedance arc at different temperatures. Arcs from grain interiors occurred in high frequency (10<sup>6</sup>–a few hundred Hz), while arcs from the grain boundaries occurred in the low frequency (a few hundred–0.1 Hz). Here, we do not consider the effects of the grain boundary conduction mechanism, since the grain interiors arcs are dominant under high-pressure conditions (Xu et al. 2000). We used a simple resistance–capacitance circuit to fit the data in order to obtain the resistance of the samples. Fitting errors are on the order of a few percent for each temperature point.

Figure 3 shows the logarithm of the electrical conductivity of dunite, lherzolite, and pyroxenite at 2–3 GPa, respectively. We can see that the electrical conductivity of

**Table 2** Water contents of individual minerals and bulk rocks

Dunite <sup>a</sup> (wt%)	Lherzolite <sup>b</sup>			Pyroxenite <sup>c</sup>	
	OI (wt%)	Cpx (wt%)	Opx (wt%)	Cpx (wt%)	Opx (wt%)
9.16E-4	1.75E-3	3.53E-2	2.81E-2	2.31E-3	5.06E-3
1.65E-3	1.76E-3	3.48E-3	2.27E-2	7.44E-3	1.14E-2
1.66E-3	2.60E-3	5.65E-2	4.82E-2	7.71E-3	1.64E-2
2.45E-3	4.59E-3	5.42E-2	6.51E-3	1.15E-2	1.88E-2
3.93E-3	5.82E-3	1.90E-3	1.01E-2	1.41E-2	2.76E-2
		1.75E-2	3.74E-2	1.78E-2	
Bulk rock water content (wt%)					
2.21E-3	1.26E-2			1.31E-2	

<sup>a</sup> Five regions of the thin section of dunite from rim to center are determined, two more grains are include in each region. The bulk water content water is the average water content of these five regions

<sup>b</sup> The bulk water content of lherzolite was calculated according to the composition of 60% OI + 25% Opx + 15% Cpx; all percentages are volume percents

<sup>c</sup> The bulk water content of pyroxenite was calculated according to the composition of 50% Opx + 50% Cpx; all percentages are volume percents

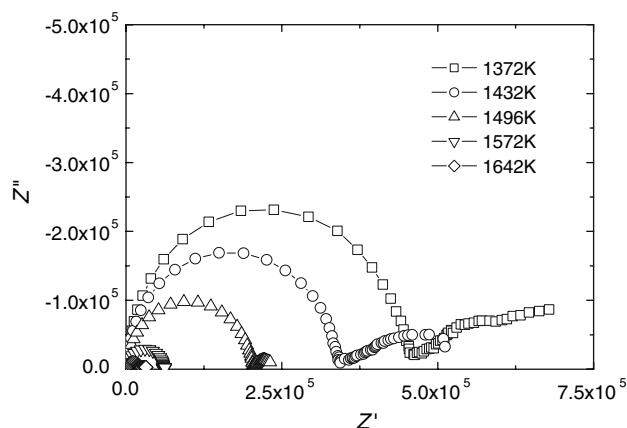


**Fig. 2** Impedance spectra of dunite at 3.0 GPa. These symbols represent impedance arcs at different temperatures. The arc’s diameter decreases as resistance decreases with increasing temperature. The real  $Z'$  and imaginary  $Z''$  parts of the impedance were obtained from the measurement of the magnitude,  $|Z|$ , and the phase angle, determined at a given frequency using the following two equations:  $Z' = |Z| \cos \theta$ ;  $Z'' = |Z| \sin \theta$ . The frequency of each data point increases from right to left along each trajectory

the three rocks depends weakly on pressure at 2.0 GPa and 3.0 GPa. The electrical conductivity of lherzolite is 0.5 orders of magnitude higher than that of dunite. The electrical conductivity of pyroxenite is one order of magnitude higher than that of dunite.

The electrical conductivity of silicate minerals and rocks is controlled by defect chemistry. It is known that the water

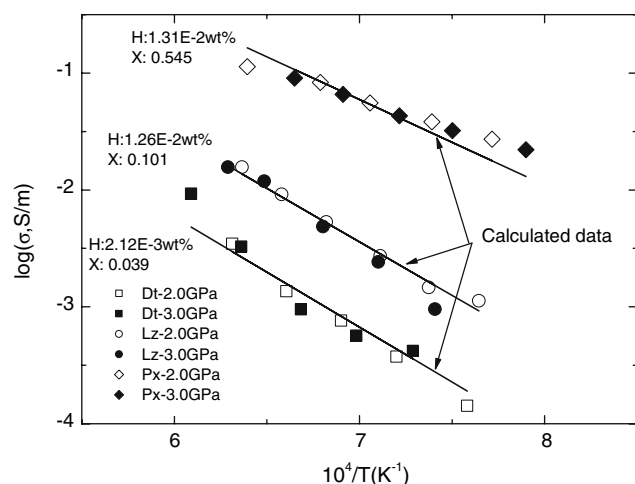


**Fig. 3** Logarithm of electrical conductivity of dunite, lherzolite, and pyroxenite at 2.0–3.0 GPa. Empty squares and solid squares represent the electrical conductivity of dunite at 2.0 GPa and 3.0 GPa, respectively. Empty circles and solid circles represent the electrical conductivity of lherzolite at 2.0 GPa and 3.0 GPa. Empty diamonds and solid diamonds represent the electrical conductivity of pyroxenite at 2.0 GPa and 3.0 GPa, respectively. Abbreviations are Dt, dunite; Lz, lherzolite; and Px, pyroxenite. The solid lines with numbers are the results of multi-linear regression from all the data; the numbers with lines are the water content (in wt%) and the iron content, Abbreviations are H, hydrogen; X, Fe/(Fe + Mg). The error bars of experimental electrical conductivity are smaller than the symbol size

(hydrogen) and iron content dramatically influence the electrical conductivity in silicate minerals and rocks. The iron dependence of electrical conductivity of nominally dry olivine has been widely studied (e.g., Lacam 1983; Omura et al. 1989; Hirsch et al. 1993). In particular, Hirsch et al. (1993) indicated that the conductivity of Fe-bearing olivine is proportional to

$$X_{\text{Fe}}^{1.8} \left( X_{\text{Fe}} = \frac{\text{Fe}}{\text{Fe} + \text{Mg}} \right).$$

However, in our cases, each of the three rocks samples has a different water and iron content; the olivine electrical conductivity model inferred by Hirsch et al. (1993) could not be used to directly interpret our electrical conductivity results from the three types of rocks we reported.

To interpret the electrical conductivity results reported in the present article, the effects of both water and iron content must be taken into account. For the present analysis, it is assumed that the dependence of electrical conductivity on water and iron content may be written as:

$$\sigma = AC_{\text{W}}^r \exp(-H^*/RT) \exp(\alpha X_{\text{Fe}}/RT) \quad (3)$$

where  $\sigma$  is electrical conductivity,  $A$  and  $\alpha$  are constants,  $H^*$  is activation enthalpy,  $R$  is the gas constant and  $T$  is temperature, and  $X_{\text{Fe}} = (\text{Fe})/(\text{Fe} + \text{Mg})$ . All the data were fitted and the results were summarized in Table 3.

**Table 3** Parameter values for electrical conductivity of dunite, pyroxenite, and lherzolite

$\text{Log}_{10} A$ (S/m)	$r$	$\alpha$ (kJ/mol)	$H^*$ (kJ/mol)
$5.2 \pm 0.4$	$0.67 \pm 0.07$	$79 \pm 3$	$183 \pm 9$

We used the bulk rocks water contents (Table 2) and  $X_{\text{Fe}}$  (Table 1) to calculate the electrical conductivity of the three types of rocks by Eq. 3 and the derived fit parameters (Table 3). The results showed that calculated values are approximately consistent with experimental values (in Fig. 3).

Some high-pressure mineral hydration experiments (Aines and Rossman 1984; Smyth et al. 1991; Bell and Rossman 1992; Kohlstedt et al. 1996) indicated that water is incorporated into common upper mantle minerals in the form of hydroxyl via substitution into Mg vacancies (2H-Mg<sup>2+</sup>). Moreover, the experimental study of partitioning of water between common upper mantle minerals (Hauri et al. 2006) indicated that incorporation of H<sub>2</sub>O into pyroxene is also accomplished by a coupled substitution in which H<sup>+</sup> and Al<sup>3+</sup> replace Si<sup>4+</sup> in the mineral structure. In addition, Hauri et al. (2006) found that coupled substitution of H<sup>+</sup> and tetrahedral Al<sup>3+</sup> dominated over 2H-Mg<sup>2+</sup> substitutions. The electrical conductivity experiments of hydrous olivine (e.g., Yoshino et al. 2006; Wang et al. 2006) and its high-pressure polymorphs (e.g., Huang et al. 2005) show that not all the hydrogen atoms in Mg (Fe) vacancies contribute to electrical conductivity and suggest the free protons escaping from the Mg (Fe) vacancies are responsible for the electrical conductivity. By analogy with olivine, we suggest that the conductivity of hydrous pyroxenes is controlled by free protons escaping from both Mg vacancies and Si vacancies. We note that in Table 3, the parameter,  $r$  ( $\sim 0.67$ ), is close to our previous results,  $r$  ( $\sim 0.62$ ) (Wang et al. 2006). This indicates that the effect of water on the electrical conductivity of these rocks is similar to that of hydrogen-rich olivine (Wang et al. 2006). However, the activation enthalpy (183 kJ/mol) is significantly higher than that of hydrogen-rich polycrystalline olivine (87 kJ/mol) derived by Wang et al. (2006) and single crystal (0.78–0.98 eV) by Yoshino et al. (2006). It is also necessary to point out that the experimental temperatures ( $\sim 1,273$ – $1,573$  K) in this study are higher than those of hydrogen-rich olivine (Wang et al. 2006; Yoshino et al. 2006), the samples may lose some water at high temperature, in this case, the small polaron corresponding to the high activation enthalpy should also play a role in the electrical conductivity of hydrous rocks. In the present analysis, the high activation enthalpy and the value of  $r$  are consistent with the mixture conduction mechanism; both

small polarons and free protons may make the contributions to conduction of the three rocks samples.

We should note that minor phases (oxides, hydrous weathered phases on grain boundaries) could make the bulk composition not representative of the olivine and pyroxene phases, but these minor phases cause only small uncertainties because the bulk composition are controlled by the olivine and pyroxene phases, moreover, hydrous weathered phase on grain boundaries, if any, have decomposed above 1,273 K. We also mention that the Fe–Mg partitioning may affect the conductivity, however, an experimental study (Hier-Majumder et al. 2005) suggests that the influence of conduction by diffusion of Mg (Fe) is small.

### Geophysical implications

We extrapolated our results in terms of temperature, iron content and water content, and compared the results with some of geophysical observations of the upper mantle (Fig. 4). We notice that geophysical observations (Schultz et al. 1993; Lizarrade et al. 1995; Utada et al. 2003) from the upper mantle above 400 km show that the electrical conductivity has a large variation. The electrical conductivity in the continental upper mantle (Schultz et al. 1993) is typically lower, on the order of  $\sim 10^{-2}$  S/m. These values correspond to a lower water content, on the order of

$\sim 10^{-3}$  wt% or less. The electrical conductivity values in the oceanic upper mantle from 200 to 400 km depth vary from  $\sim 10^{-3}$  to  $10^{-1}$  S/m (Lizarrade et al. 1995; Utada et al. 2003). In contrast, the estimated water content in the oceanic upper mantle, according to our results, is from almost  $\sim 10^{-3}$  wt% to  $\sim 9 \times 10^{-2}$  wt% which corresponds to a variation in conductivity of a factor of  $\sim 10^2$ . The electrical conductivity peak of 0.1 S/m at the depth range 200–250 km (Lizarrade et al. 1995) corresponds to the maximum water content ( $9 \times 10^{-2}$  wt%). These results indicated that our water-induced enhancement of conductivity model could explain the conductivity anomaly in the oceanic upper mantle without involving the presence of partial melt at these depths. The average water content in the upper mantle estimated from Lizarrade's model (1995) agrees approximately with the estimated values of water content from the H<sub>2</sub>O partitioning in upper mantle minerals (Hauri et al. 2006).

The maximum water content inferred from this study was higher than that estimated from the electrical conductivity models of olivine alone (Yoshino et al. 2006; Wang et al. 2006). The main difference may result from the fact that we took into account the effect of pyroxene in the new model. The bulk mantle conductivity is dominated by the conductivity of pyroxenes because water solubility in pyroxenes is significantly higher than that of olivine in the upper mantle.

We conclude that the electrical conductivity differences between the specimens of dunite, lherzolite, and pyroxenite at the same pressure, temperature and oxygen fugacity may arise from the iron and water content. The effect of iron and water content on electrical conductivity can be described by the equation,

$$\sigma = 10^{5.2 \pm 0.4} C_W^{0.67 \pm 0.07} \exp\left(-\frac{(183 \pm 9)\text{kJ/mol}}{RT}\right) \times \exp\left(X_{\text{Fe}} \frac{(79 \pm 3)\text{kJ/mol}}{RT}\right).$$

A comparison of the laboratory data with geophysical observations show that the water content is well constrained by the conductivity data, which will provide us with a clue to a number of geodynamic processes occur in the upper mantle.

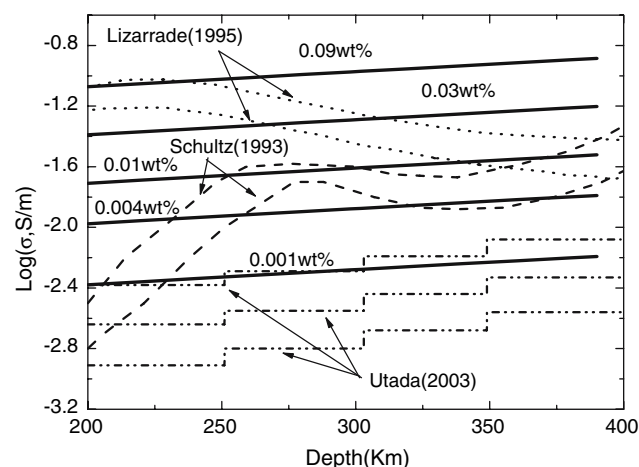


**Fig. 4** Comparison of experimental conductivity model with geophysically observed electrical conductivity models. Broken dotted lines are the magnetotelluric/geomagnetic data from Northeastern Pacific mantle (Lizarrade et al. 1995), broken short-dashed lines from the central Canadian shield (Schultz et al. 1993) and broken dash-dot-dotted lines from the north Pacific region (Utada et al. 2003). Solid lines show the conductivity values calculated from the model:  $\sigma = 10^{5.2 \pm 0.4} C_W^{0.67 \pm 0.07} \exp\left(-\frac{(183 \pm 9)\text{kJ/mol}}{RT}\right) \exp\left(X \frac{(79 \pm 3)\text{kJ/mol}}{RT}\right)$ . We assume that  $X$ , the ratio of Fe/(Fe + Mg), is 0.1, which is thought to be the average composition in the upper mantle. The numbers with lines indicate the water content (in wt%)

**Acknowledgments** We acknowledge Karato S-I and Xu Y-S for their fruitful discussions. The manuscript benefited from constructive reviews by two anonymous reviewers. This work was supported by National Natural Science Foundation of China (40774036, 40574022); the special grant from the president of Chinese Academy of Sciences and Graduate University of Chinese Academy Sciences; the basic research program from Institute of Earthquake Science, China Earthquake Administration (02076902-33); one hundred individual project of Chinese Academy of Sciences (M2055) and important field program of Knowledge Innovation Program (KZCX3-SW-124).

## References

- Aines RD, Rossman GR (1984) Water content of mantle garnets. *Geology* 12:720–723
- Akella J, Kennedy GC (1971) Melting of gold, silver and copper proposal for a new high-pressure calibration scale. *J Geophys Res* 76:4969–4977
- Akimoto S, Yagi T, Inoue K (1977) High temperature-pressure phase boundaries in silicate system using in situ X-ray diffraction. In: Manghani M, Akimoto S (eds) High-pressure research application in geophysics. Academic Press, New York, pp 585–602
- Bai Q, Kohlstedt DL (1992) Substantial hydrogen solubility in olivine and implications for water storage in the mantle. *Nature* 357:672–674
- Bell DR, Rossman GR (1992) Water in Earth's mantle: the role of nominally anhydrous minerals. *Science* 255:1391–1397
- Hauri EH, Gaetai GA, Green TH (2006) Partitioning of water during melting of the Earth's upper mantle at H<sub>2</sub>O-undersaturated conditions. *Earth Plane Sci Lett* 248:715–734
- Hier-Majumder S, Anderson IM, Kohlstedt DL (2005) Influence of protons on Fe–Mg inter-diffusion in olivine. *J Geophys Res* 110, doi:10.1029/2004JB003292
- Hirsch LM, Shankland TJ, Duba AG (1993) Electrical conductivity and polaron mobility in Fe-bearing olivine. *Geophys J Int* 114:36–44
- Hirschmann MM, Aubaud C, Withers AC (2005) Storage capacity of H<sub>2</sub>O in nominally anhydrous minerals in the upper mantle. *Earth Planet Sci Lett* 236:167–181
- Huang XG, Xu YS, Karato SK (2005) Water content in the transition zone from electrical conductivity of wadsleyite and ringwoodite. *Nature* 434:746–749
- Irfune T, Ringwood AE (1987) Phase transformations in primitive MORB and pyrolite compositions to 25 GPa and some geophysical implications. In: Manghani MH and Syono Y (eds) High pressure research in mineral physical. AGU, Washington, DC. *Geophys Monogr Ser* 39:231–242
- Karato S (2003) Mapping water content in the upper mantle. In: Eiler J (ed) Inside the subduction factory. AGU, Washington, DC. *Geophys Monogr* 138:135–152
- Karato S (2006) Remote sensing of hydrogen in Earth's mantle reviews in mineralogy & geochemistry. In: Keppler H, Smyth (eds) Water in nominally anhydrous minerals, vol 62, pp 343–375
- Kohlstedt DL, Keppler H, Rubie DC (1996) Solubility of water in the  $\alpha$  and  $\beta$ : phases of (Mg, Fe)<sub>2</sub>SiO<sub>4</sub>. *Contrib Mineral Petrol* 123:345–357
- Lacam A (1983) Pressure and composition dependence of the electrical conductivity of iron-rich synthetic olivine to 200 kbar. *Phys Chem Miner* 9:127–132
- Lizaralde D, Chave A, Hirth G, Schultz A (1995) Northeastern Pacific mantle conductivity profile from long-period magnetotelluric sounding using Hawaii-to California submarine cable data. *J Geophys Res* 100: 17837–17854
- Omura K, Kurita K, Kumazawa M (1989) Experimental study of pressure dependence of electrical conductivity of olivine at high temperature. *Phys Earth Planet Inter* 57:291–303
- Paterson MS (1982) The determination of hydroxyl by infrared absorption in quartz, silicate glass and similar materials. *Bull Mineral* 105:20–29
- Ringwood AE (1975) Composition and petrology of the earth's mantle. McGraw-Hill, New York
- Roberts JJ, Tyburczy JA (1991) Frequency dependent electrical properties of polycrystalline olivine compacts. *J Geophys Res* 96:16, 205–216, 222
- Rudnick RL, Gao S, Ling W (2004) Petrology and geochemistry of spinel peridotite xenoliths from Hannuba and Qixia, North China craton. *Lithos* 77:609–637
- Schultz A, Kurtz RD, Chave AD et al (1993) Conductivity discontinuities in the upper mantle beneath a stable craton. *Geophys Res Lett* 20:2941–2944
- Smyth JR, Bell DR, Rossman GR (1991) Hydroxyl in upper mantle clinopyroxenes. *Nature* 35:732–735
- Tyburczy JA, Roberts JJ (1990) Low frequency electrical response of polycrystalline olivine compacts: grain boundary transport. *Geophys Res Lett* 17:1985–1988
- Utada H, Koyama T, Shimizu H, Chave AD (2003) A semi-global reference model of electrical conductivity in the mid-mantle beneath the north Pacific region. *Geophys Res Lett* 30, doi:10.1029/2002GL016092
- Wang D, Mookherjee M, Xu Y, Karato S (2006) The effect of water on electrical conductivity of olivine. *Nature* 443:977–980
- Williams Q, Hemley RJ (2001) Hydrogen in the deep earth. *Annu Rev Earth Planet Sci* 29:365–418
- Xu Y-G (2002) Evidence for crustal components in the mantle and constraints on crustal recycling mechanisms: pyroxenite xenoliths from Hannoba, North China. *Chem Geol* 182:301–322
- Xu J, Zhang Y, Hou W (1994) Measurements of ultrasonic wave velocity at high temperature and high pressure for window glass pyrophyllite and kimberlite up to 1400 L and 5.5GPa. *High-temp High-press* 26:375–384
- Xu Y-S, Poe BT, Shankland TS (1998) Electrical conductivity of olivine, wadsleyite, and Ringwoodite under upper-mantle conditions. *Science* 280:1415–1418
- Xu Y-S, Shankland TJ, Duba AG (2000) Pressure effect on electrical conductivity of mantle olivine. *Phys Earth Planet Inter* 118:149–161
- Yoshino T, Matsuzaki T, Yamashita S et al (2006) Hydrous olivine unable to account for conductivity anomaly at the top of the asthenosphere. *Nature* 443:973–976